



GLOBAL JOURNAL OF RESEARCHES IN ENGINEERING: F  
ELECTRICAL AND ELECTRONICS ENGINEERING  
Volume 22 Issue 2 Version 1.0 Year 2022  
Type: Double Blind Peer Reviewed International Research Journal  
Publisher: Global Journals  
Online ISSN: 2249-4596 & Print ISSN: 0975-5861

# AFIS based Advanced Power Control Scheme for Grid-Connected DFIG-Driven WECS

By Ifte Khairul Amin & M. Nasir Uddin

*Shahjalal University of Science & Technology*

**Summary-** In wind energy conversion system, extraction of optimum power and efficient operation are two major challenges. In grid connected mode, a doubly fed induction generator (DFIG) control unit is designed to operate at optimum speed to deliver maximum output power in the grid while the voltage, frequency and harmonic regulations need to be fulfilled. Vector control associated with proportional-integral (PI) controllers has been widely applied in wind farms for reliable power regulation of DFIG. As DFIG based wind energy conversion system (WECS) experiences strong nonlinearity and uncertainties originated from the aerodynamics of the wind turbine and magnetic saturation of the generator, different adaptive and nonlinear control schemes have been proposed to resolve the problems associated with fixed-gain PI controllers.

**Keywords:** *on-line tuning, AFIS control, doubly fed induction generator, wind energy conversion system, power control.*

**GJRE-F Classification:** *DDC Code: 621.312136 LCC Code: TJ820*



*Strictly as per the compliance and regulations of:*



© 2022. Ifte Khairul Amin & M. Nasir Uddin. This research/review article is distributed under the terms of the Attribution-NonCommercial-NoDerivatives 4.0 International (CC BYNCND 4.0). You must give appropriate credit to authors and reference this article if parts of the article are reproduced in any manner. Applicable licensing terms are at <https://creativecommons.org/licenses/by-nc-nd/4.0/>.

# AFIS based Advanced Power Control Scheme for Grid-Connected DFIG-Driven WECS

Ifte Khairul Amin <sup>α</sup> & M. Nasir Uddin <sup>σ</sup>

**Summary-** In wind energy conversion system, extraction of optimum power and efficient operation are two major challenges. In grid connected mode, a doubly fed induction generator (DFIG) control unit is designed to operate at optimum speed to deliver maximum output power in the grid while the voltage, frequency and harmonic regulations need to be fulfilled. Vector control associated with proportional-integral (PI) controllers has been widely applied in wind farms for reliable power regulation of DFIG. As DFIG based wind energy conversion system (WECS) experiences strong nonlinearity and uncertainties originated from the aerodynamics of the wind turbine and magnetic saturation of the generator, different adaptive and nonlinear control schemes have been proposed to resolve the problems associated with fixed-gain PI controllers. Among adaptive controllers, adaptive fuzzy inference system (AFIS) has the distinguishing feature of modeling a highly nonlinear system and adopting the uncertainties. Hence; in this paper, an AFIS based NFC controller is proposed to regulate the converters of grid-connected DFIG. The proposed algorithm is tested for variable wind speed conditions and the results are compared with fixed gain PI controller and adaptive back-stepping based nonlinear controller. The simulation results suggest that the proposed scheme shows excellent adaptation with the variable condition through the change of its parameters and comparatively better performance in terms of speed and current tracking.

**Keywords:** on-line tuning, AFIS control, doubly fed induction generator, wind energy conversion system, power control.

*List of Symbols and Abbreviations:*

$v_{ds}, v_{qs}, v_{dr}, v_{qr}, v_{dc}, v_{qc}$  —d-q axis stator, rotor, grid converter voltages (V)

$i_{ds}, i_{qs}, i_{dr}, i_{qr}, i_{dc}, i_{qc}$  — d-q axis stator, rotor, grid converter currents (A)

$R_s, R_r$ — Stator, rotor and core loss resistances ( $\Omega$ )

$\omega_s, \omega_r$ —synchronous and rotor electrical angular speed (rad/s)

$P$ —Number of pole pairs

$L_s = L_{\sigma s} + L_m$  —Stator self-inductance (H)

$L_r = L_{\sigma r} + L_m$  —Rotor self-inductance (H)

$L_{\sigma s}, L_{\sigma r}$ — Stator and rotor leakage inductances (H)

$L_m$ — Magnetizing inductance (H)

$T_e$ -Electromagnetic developed torque (N-m)

$Q_s, Q_{grid}$  — Reactive power in the stator side and grid

$T_t$ - Turbine torque (N-m)

$V_{bus}$  – Bus voltage

$V_{grid}$  -Grid voltage

## I. INTRODUCTION

Among the major challenges of WECS, controlled extraction of power from intermittent generation and supervision on nonlinear system dynamics of DFIG-WECS are of critical importance. Different optimum point search algorithms have been proposed in [1-5] to find out the peak power generated by the WECS. The conventional vector control scheme involves cascaded control loops where simple proportional-integral (PI) controllers are executed to regulate the voltage/current [6-8]. The fixed gain PI controllers may fail to implement proper tracking performance if the constants are not selected appropriately. Furthermore, the performance of the PI controller deteriorates with the variation in machine parameters due to the change in temperature, magnetic saturation and machine-aging. Since DFIG inherits nonlinear magnetization characteristics, nonlinear control techniques are adopted to achieve enhanced dynamic behavior for the control operation of the system. Hence, the researchers have focused on more sophisticated problems for WECS control, such as backstepping based nonlinear control [9], fuzzy logic control [10], sliding mode control [11] etc. The major drawback of the reported fuzzy inference system is that it is completely based on the knowledge and experience of the designer [12]. Intelligent control algorithms such as neural network (NN)[13], neuro-fuzzy control (NFC)[14], adaptive network-based fuzzy inference system (ANFIS)[15], genetic algorithm[16], particle swarm optimization[17], artificial bee colony algorithm[18], grey wolf optimization[19] have been gaining popularity over the last decade. Among the intelligent control algorithm, AFIS combines the competence of fuzzy reasoning in handling uncertainties and learning aptitude of adaptive network from complex system. Also, the algorithm is capable to model the nonlinear features of a system. Therefore, an AFIS based NFC controller is designed for converter control for real and reactive power control of grid-connected DFIG based WECS to extract maximum power from the wind. The performance of the AFIS controller has been investigated with the fixed gain PI and adaptive backstepping based nonlinear controllers under various operating conditions. The simulation

*Author α:* Associate Professor, Department of EEE, Shahjalal University of Science & Technology, Sylhet, Bangladesh.

e-mail: iam@lakeheadu.ca

*Author σ:* Department of Electrical Engineering, Lakehead University, Barrie, Ontario, Canada.

results demonstrate the efficacy of the AFIS algorithm over other controllers for its intelligent pattern recognition scheme.

## II. PROPOSED CONFIGURATION OF THE SYSTEM

In the proposed configuration, the DFIG is mechanically coupled with the turbine to transform the mechanical energy into electrical energy. A back-to-back converter is implanted to perform independent control of DC-link voltage and decoupled control of real and reactive power. Separate control circuits are required to regulate the grid-side converter (GSC) and rotor side converter (RSC) as shown in Fig. 1. Adaptive

fuzzy scheme with on-line tuning feature is implemented to design the proposed controllers. The turbine, DFIG and grid parameters are shown in Table 1.

### a) AFIS Structure

AFIS can be considered as an intelligent and powerful processing tool for pattern recognition and controller design because it combines the advantages of both the fuzzy logic and online parameter adaptation. The following subsections illustrate the structure of AFIS network and demonstrate the AFIS based controller configuration of the DFIG-WECS primarily linked with grid.

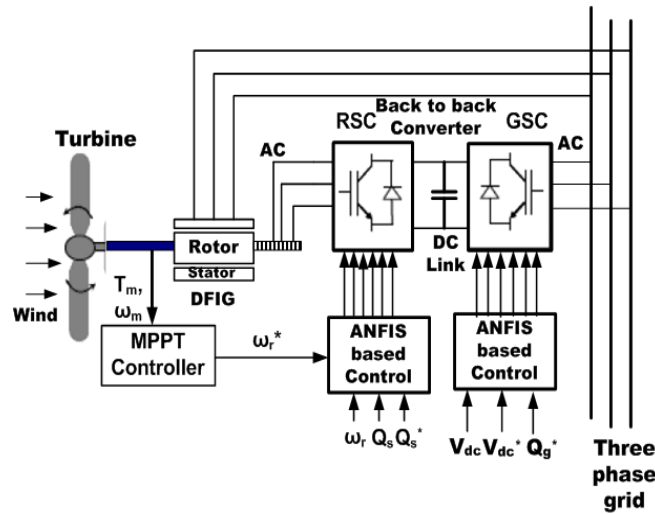


Fig. 1: Full configuration of the proposed AFIS controller based DFIG-WECS

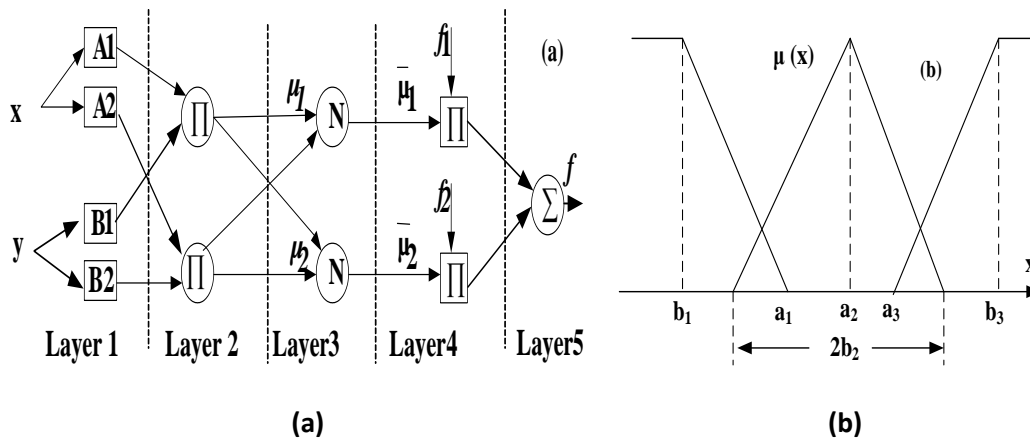


Fig. 2: (a) Schematic of AFIS architecture (b) Membership function for input data x

### i. AFIS Layers

Adaptive fuzzy inference system consists of a fuzzy inference system whose membership functions can be reconstructed by using an authentic input-output data set. The parameters associated with the membership functions are obtained by gradient descent algorithm. When the gradient vector is determined, it utilizes least square error calculation method to adjust

the parameters to reduce the error function. AFIS networks usually utilize a combination of least squares estimation and back propagation for membership function parameter estimation. The details of AFIS structure can be found in [20, 21].

The controller for the converters is designed by utilizing fuzzy logic and adaptive neural network algorithms. AFIS can be considered as an intelligent

and powerful processing tool for pattern recognition and controller design because it combines the advantages of both the fuzzy logic and neural network algorithms. The parameters associated with the membership functions are updated by gradient descent algorithm. When the gradient vector is determined, it utilizes one of its optimization techniques to adjust the parameters to reduce the error function. AFIS networks usually utilize a combination of least squares estimation and back propagation for membership function parameter estimation. Fig. 2(a) and 2(b) illustrates a generalized configuration and membership function for the proposed AFIS network, respectively. The description of each layer in the AFIS structure is explained in the following section.

**Layer 1:** The first layer is also known as the fuzzification layer, a number of membership functions are assigned to each input. Only one input is used in this layer which is the normalized error function of bus voltage ( $V_{bus}$ ), rotor speed ( $\omega_r$ ), reactive power ( $Q_s$ ) based on the converter control.

$$x = \frac{\alpha - \alpha_{ref}}{\alpha_{rated}} \tag{1}$$

Here,  $\alpha = \omega_r, V_{bus}$  or  $Q_s$ .

The membership functions are defined in this stage. The equations for the membership function are defined in (2-4).

$$\mu_{A1}^1(x) = \begin{cases} 1, & x \leq b_1 \\ \frac{x-a_1}{b_1-a_1}, & b_1 < x < a_1 \\ 0, & x \geq a_1 \end{cases} \tag{2}$$

$$\mu_{A2}^2(x) = \begin{cases} 0, & |x| \geq b_2 \\ 1 - \frac{|x-a_2|}{b_2}, & |x| < b_2 \end{cases} \tag{3}$$

$$\mu_{A3}^3(x) = \begin{cases} 0, & x \leq a_3 \\ \frac{x-a_3}{b_3-a_3}, & a_3 < x < b_3 \\ 1, & x \geq b_3 \end{cases} \tag{4}$$

where, x is the input for the membership function calculation block,  $a_1, b_1, a_2, b_2, a_3$  and  $b_3$  are the parameters defined in the corresponding membership function which needs to be tuned during control action. The parameter  $a_2$  is selected as zero to reduce the computational burden.

**Layer 2:** In this layer, each node multiplies the entering signals and directs the output to the next level that represents the individual firing strength  $\mu_i$  of a rule.

$$\mu_i = \mu_{A1}^i(x)\mu_{A2}^i(x)\mu_{A3}^i(x) \tag{5}$$

For the proposed controller only one input is chosen. So, the second layer can be ignored and the output of first layer goes to the third layer.

$$\mu_1 = \mu_{A1}^1(x), \mu_2 = \mu_{A2}^2(x), \mu_3 = \mu_{A3}^3(x) \tag{6}$$

**Layer 3:** Each block in the third layer which is also known as normalization stage, estimates the proportion of the i-th rule firing strength ( $\bar{\mu}_i$ ) to the sum of the firing strength of all rules.

$$\bar{\mu}_i = \frac{\mu_i}{\mu_1 + \mu_2 + \mu_3} \tag{7}$$

**Layer 4:** In this layer, the function,  $f_i$  is calculated as the linear activation function. A single input first order Sugeno fuzzy model is utilized in this model.

$$f_1 = \beta_0^1 + \beta_1^1 x \tag{8}$$

$$f_2 = \beta_0^2 + \beta_1^2 x \tag{9}$$

$$f_3 = \beta_0^3 + \beta_1^3 x \tag{10}$$

In this stage, the parameters  $\beta_0, \beta_1$  are tuned based on the operating condition of DFIG. These parameters are known as consequent parameters.

**Layer 5:** The final layer is the output layer which computes the overall output by combining the incoming data.

$$f = \bar{\mu}_1 f_1 + \bar{\mu}_2 f_2 + \bar{\mu}_3 f_3 \tag{11}$$

ii. *Online self-tuning algorithm*

It is impossible to calculate the desired outputs of the AFIS controller for all possible conditions, which are d-q axis currents for rotor and grid side control ( $i_{dr}, i_{qr}, i_{dg}, i_{qg}$ ). Hence training data sequence can't be obtained especially for variable wind speed. Therefore, an unsupervised self-tuning algorithm is developed in the paper. The controller targets to minimize the objective function which is a squared normalized error function of the AFIS controller input. The objective function is defined as,

$$W = \frac{1}{2} e^2 = \frac{1}{2} \left( \frac{x^* - x}{x_{rated}} \right)^2 \tag{12}$$

where  $x^*, x$  and  $x_{rated}$  are the reference, actual and desired value of the variable and x is scalar.

iii. *Tuning of Pre-Condition and Consequent Parameters*

The learning rule of the proposed controller can be given as [22]:

$$a_i(n+1) = a_i(n) - \gamma_{ai} \frac{\partial W}{\partial a_i}, b_i(n+1) = b_i(n) - \gamma_{bi} \frac{\partial W}{\partial b_i} \tag{13}$$

Where,  $\gamma_{ai}$  and  $\gamma_{bi}$  are the learning rates of the corresponding parameters. The derivatives can be defined as:

$$\frac{\partial W}{\partial a_i} = \frac{\partial W}{\partial e} \frac{\partial e}{\partial x} \frac{\partial x}{\partial f} \frac{\partial f}{\partial \mu_{Ai}^i} \frac{\partial \mu_{Ai}^i}{\partial a_i}, \quad \frac{\partial W}{\partial b_i} = \frac{\partial W}{\partial e} \frac{\partial e}{\partial x} \frac{\partial x}{\partial f} \frac{\partial f}{\partial \mu_{Ai}^i} \frac{\partial \mu_{Ai}^i}{\partial b_i} \quad (14)$$

Now we get,  $\frac{\partial W}{\partial e} = e = \frac{x^* - x}{x_{rated}}$ ,  $\frac{\partial e}{\partial x} = -\frac{1}{x_{rated}}$  and  $\frac{\partial x}{\partial f} = J$ , assuming J is the Jacobian matrix of the system. It is very difficult to determine system's Jacobian matrix. For decoupled control of DFIG, the system is assumed as a single input single output system and then the Jacobian matrix is considered as a positive constant. Considering that the effect of J is included in tuning rate parameter, the update rule for the consequent parameter is given as:

$$a_1(n+1) = a_1(n) - \gamma_{a1} e(n) \frac{f_1(n)}{\sum \mu_{A1}^1} \frac{1 - \mu_{A1}^1(n)}{b_1(n) - a_1(n)} \quad (15)$$

$$b_1(n+1) = b_1(n) - \gamma_{b1} e(n) \frac{f_1(n)}{\sum \mu_{A1}^1} \frac{\mu_{A1}^1(n)}{b_1(n) - a_1(n)} \quad (16)$$

$$b_2(n+1) = b_2(n) + \gamma_{b2} e(n) \frac{f_2(n)}{\sum \mu_{A2}^2} \frac{1 - \mu_{A2}^2(n)}{b_2(n)} \quad (17)$$

$$a_3(n+1) = a_3(n) - \gamma_{a3} e(n) \frac{f_3(n)}{\sum \mu_{A3}^3} \frac{1 - \mu_{A3}^3(n)}{b_3(n) - a_3(n)} \quad (18)$$

$$b_3(n+1) = b_3(n) - \gamma_{b3} e(n) \frac{f_3(n)}{\sum \mu_{A3}^3} \frac{\mu_{A3}^3(n)}{b_3(n) - a_3(n)} \quad (19)$$

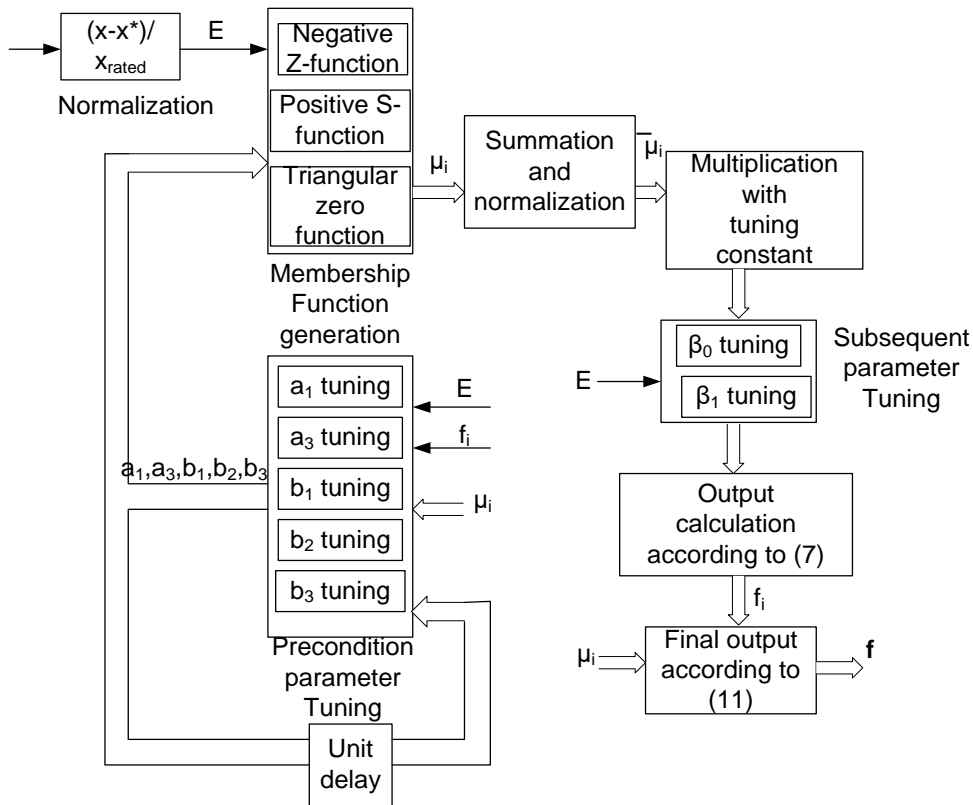


Fig. 3: Output calculation by implementing AFIS algorithm

Similarly, the update laws for tuning the consequent parameters can be derived as follows.

$$\beta_0^i(n+1) = \beta_0^i(n) - \gamma_{\beta_0^i} \frac{\partial W}{\partial \beta_0^i} \quad (20)$$

$$\beta_1^i(n+1) = \beta_1^i(n) - \gamma_{\beta_1^i} \frac{\partial W}{\partial \beta_1^i} \quad (21)$$

$\gamma_{\beta_0^i}$  and  $\gamma_{\beta_1^i}$  are the learning rates for the consequent parameters. As discussed in the update laws of

precondition parameters, the derivatives can be found from the chain rules.

$$\beta_0^i(n+1) = \beta_0^i(n) - \gamma_{\beta_0^i} e(n) \frac{f_i(n)}{\sum \mu_{Ai}^i} \frac{\mu_i}{\mu_1 + \mu_2 + \mu_3} \quad (22)$$

$$\beta_1^i(n+1) = \beta_1^i(n) - \gamma_{\beta_1^i} e(n) \frac{f_i(n)}{\sum \mu_{Ai}^i} \frac{\mu_i x}{\mu_1 + \mu_2 + \mu_3} \quad (23)$$

Finally, the output (f) will be calculated according to (7)-(11). Fig. 3 shows the parameter update mechanism for the proposed AFIS based configuration.

### III. RSC CONTROL

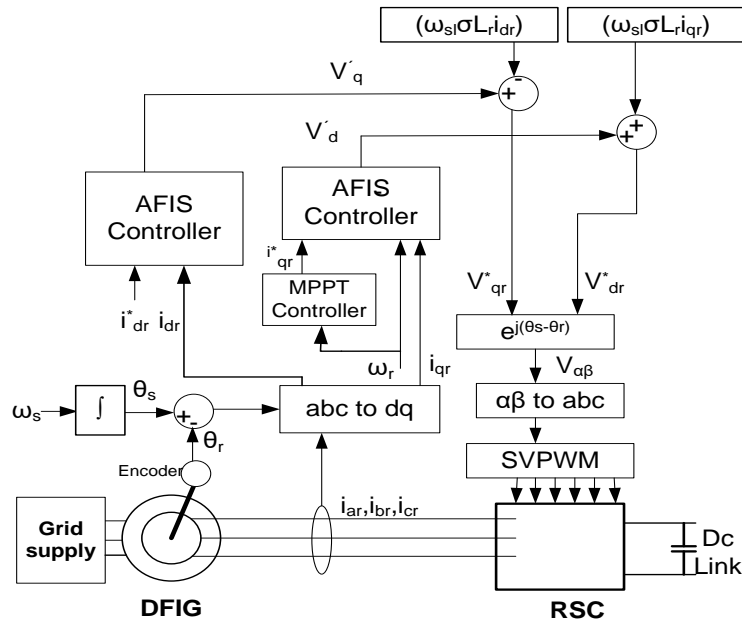


Fig. 4: AFIS architecture based RSC control for grid-connected mode of DFIG

The rotor side converter magnetizes the machine through the rotor side converter. Fig. 4 shows the RSC control scheme using the proposed AFIS architecture for grid connected DFIG. As DFIG provides decoupled control of real and reactive power, two different AFIS structures have been employed to generate the reference d-axis and q-axis rotor voltages ( $v_{dr}^*$  and  $v_{qr}^*$ ).

### IV. GSC CONTROL BY AFIS CONTROLLER

The grid side converter maintains the dc-link voltage constant irrespective of the value and direction of the rotor power flow. The AFIS controller-based configuration is implemented in GSC control to regulate the dc-link voltage as depicted in Fig. 5. The reference q-axis grid current component can be obtained from the reactive power according to (24).

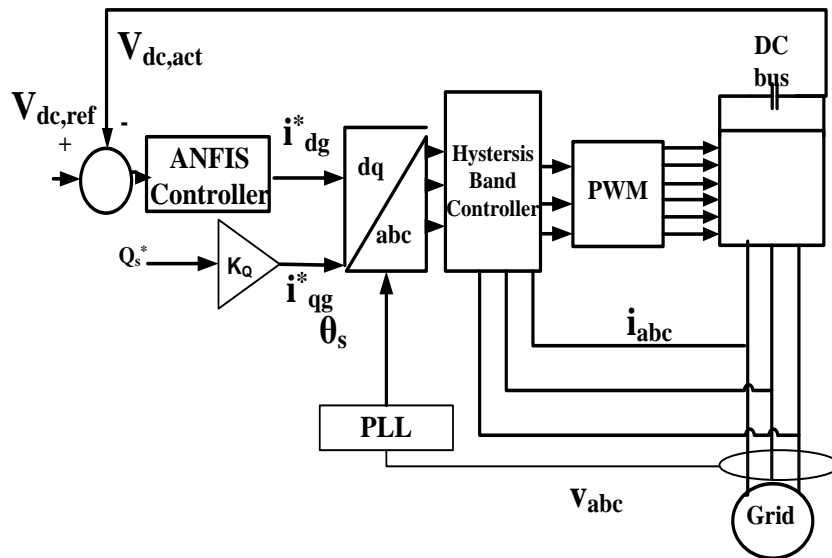


Fig. 5: AFIS based GSC control for DFIG-WECS



$$i_{qg}^* = K_Q Q_s^* = \frac{Q_s^*}{-3/2V_{grid}} \quad (24)$$

The objective function of the AFIS controller will ensure that the bus voltage error is converged to zero.

## V. PERFORMANCE ANALYSIS OF THE PROPOSED SCHEME

Speed and direction of wind at a location vary randomly with time. Therefore, the adaptability of controller is critical for wind power generators to operate effectively. AFIS based controllers have the unique property of handling uncertainty and fast convergence in varying condition. In this paper, the efficacy of the AFIS controlled RSC for grid connected DFIG is observed under variable wind speed as shown in Fig. 6.

The wind speed variation is depicted in Fig. 6(a). It is found that the AFIS controlled RSC tracks the rotor speed of the generator as dictated by the MPPT control algorithm (Fig. 6(b)). It also regulates the d-q axis rotor currents according to the demanded value to control the real and reactive power of the generator (Fig. 6(c,d)). Similarly, the GSC is controlled by the AFIS based controller which regulates the d-q axis grid current components. The bus voltage regulation performance is depicted in Fig. 6(e). It is found that the AFIS controller is capable to maintain the dc-link voltage to the reference set point which is 1150 V. A hysteresis current controller generates the control pulses for the grid converter. The current d-q axis grid current components and the three phase currents are shown in Fig. 6 (f,g,h).

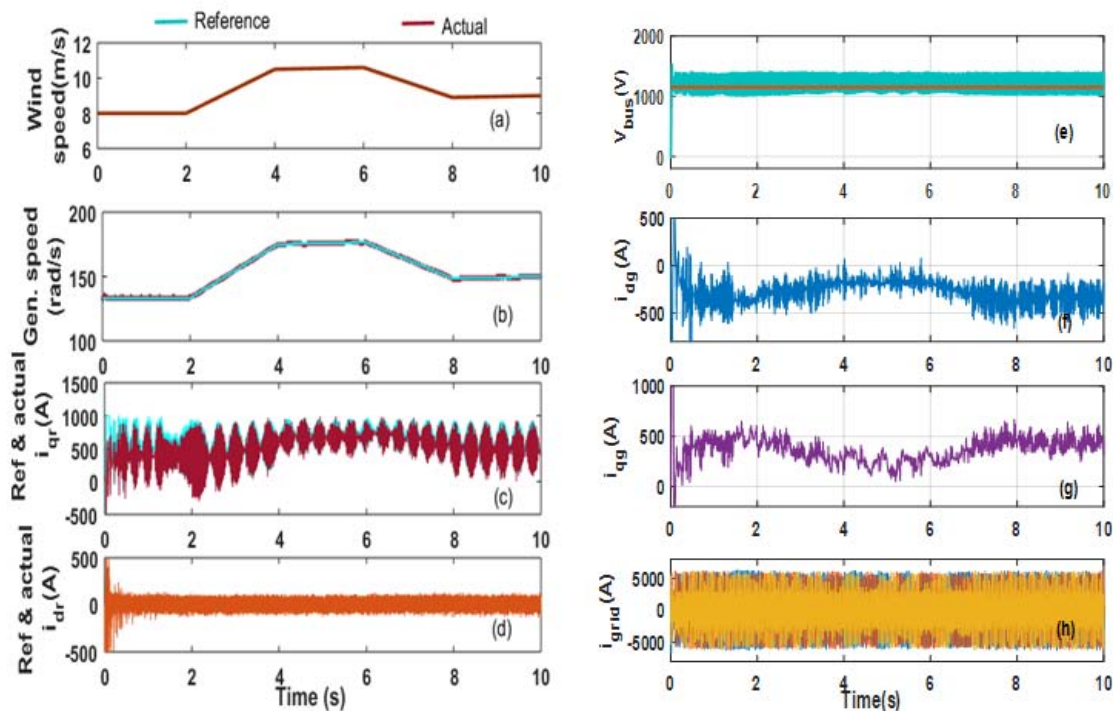


**Fig. 6:** Performance of the AFIS based RSC and GSC control: (a) Variation in wind speed, (b) Corresponding change in generator speed, (c) Reference and actual q-axis rotor current, (d) Reference and actual d-axis rotor current, (e) Reference and actual DC-link voltage, (f) d-axis grid current component, (g) q-axis grid current component, (h) Three phase grid currents.

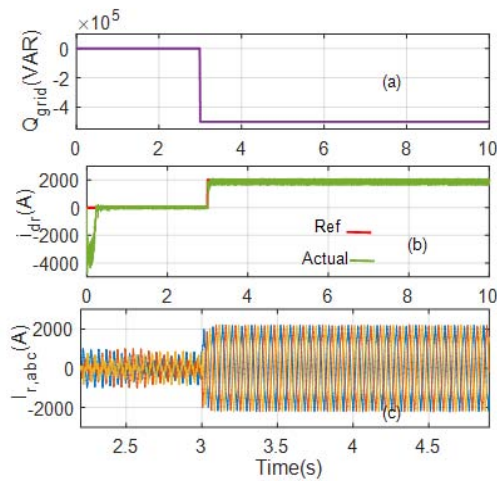


Fig. 7: AFIS based controller performance for step change in reactive power: (a) Variation in reference value of reactive power, (b) Corresponding change in reference and actual d-axis rotor currents, (c) Three phase rotor currents.

In DFIG, it is possible to control the reactive power requirement from RSC. Fig. 7 shows the feature for the proposed controller. The reference reactive power is varied from 0 to -0.5 MVAR by employing step function (Fig. 7(a)). The desired value of d-axis rotor current follows the variation of the reactive power and the actual current component successfully can follow the trajectory of the reference current as observed in Fig. 7(b) and the three phase rotor currents also change accordingly (Fig. 7(c)). The reactive power regulation proves the accuracy and effectiveness of the AFIS structure-based controller in grid-connected DFIG based WECS.

The performance of the grid connected DFIG-WESC has been investigated for conventional PI, nonlinear and AFIS based controllers under various operating conditions. First, the simulation is performed for a step change in wind speed from 6m/s to 8 m/s for each controller. The results are shown in Fig. 8. It is

observed from this figure that the PI controller has the largest overshoot and steady-state ripple compared to the other two controllers. In the PI controllers, the proportional and integral constants are selected according to Table 2. The values are calculated according to the DFIG, grid and turbine parameters [6]. The AFIS controller shows excellent speed tracking in terms of steady state error although the settling time is a bit higher than the nonlinear controller. The nonlinear controller for the comparative analysis is derived from the machine motion equation to stabilize the rotor actual speed at the reference rotor speed. The subsystem equations are exploited, and new controllers are derived by defining appropriate Lyapunov function progressively. The process terminates when the control equations for the reference voltages are derived. Backstepping based control approach is adopted to obtain the control laws for the rotor side converter control. The detailed model and equations for the proposed adaptive Lyapunov stability criterion based nonlinear controller can be found in [23,24].

Table 2: PI controller constants for comparative analysis

Rotor side PI controller parameters	Stator side PI controller parameters
$k_{p,idr} = k_{p,iqr}$ $= 2\omega_{idr} \sigma L_r - R_r$ $k_{i,idr} = k_{i,iqr} = \omega_{idr}^2 \sigma L_r$ $k_{p,\omega r} = 2\omega_b J / P$ $k_{i,\omega r} = \omega_b^2 J / P$ $\omega_{idr} = 100 \times \frac{1}{t_{ca}}$ $t_{ca} = \frac{\sigma L_r}{R_r}$ $\omega_b = \frac{1}{t_{cb}}, t_{cb} = 0.005$	$k_{p,vbus} = -10^4$ $k_{i,vbus} = -3 \times 10^5$ $k_{p,icd} = k_{p,icq} = 2\omega_{ic} L_g - R_g$ $k_{i,icd} = k_{i,icq} = \omega_{ic}^2 L_g$ $\omega_{ic} = 2\pi f_s$

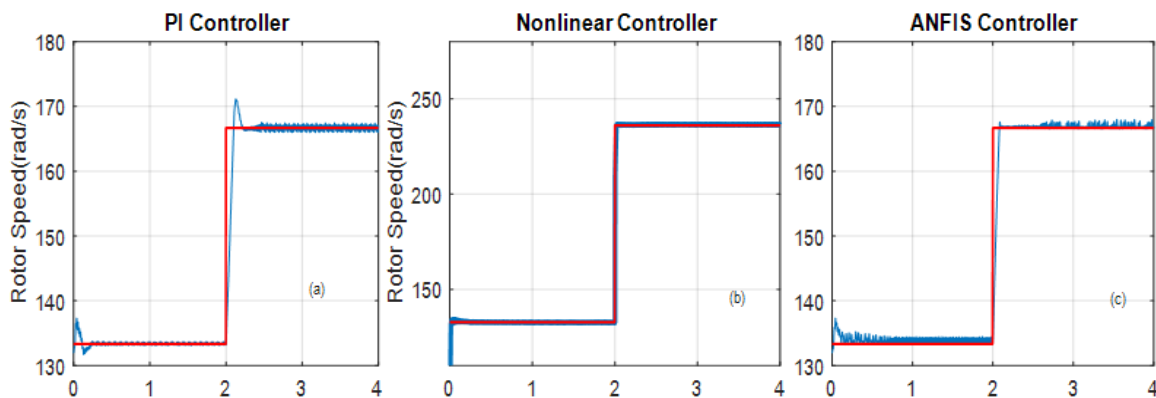


Fig. 8: Comparative rotor speed response for a step increase in wind speed: (a) PI, (b) Nonlinear, (c) AFIS



The dc-link voltage tracking performance of the controllers is also compared and shown in Figs. 9 (a)-(c). The adaptive backstepping based nonlinear

controller has very high ripples in dc-link voltage while the AFIS based controller shows the most satisfactory performance in voltage tracking.

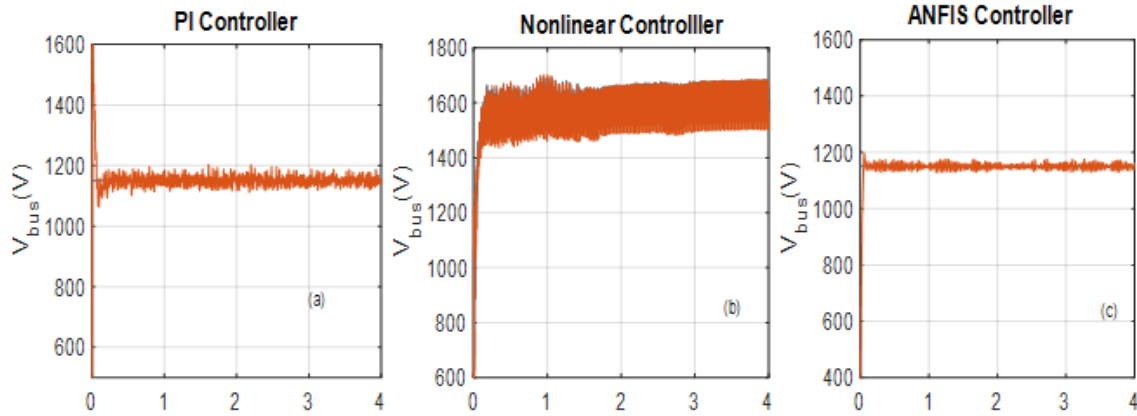


Fig. 9: Comparative dc-link voltage tracking performance at variable wind speed: (a)PI, (b) Nonlinear, (c) AFIS

Similarly, d-axis rotor current responses are investigated in Fig. 10 for a step change in reactive power demand. The PI controller shows fast current tracking while the nonlinear controller displays current

tracking with large steady state error. The proposed AFIS controller performer in between these two configurations.

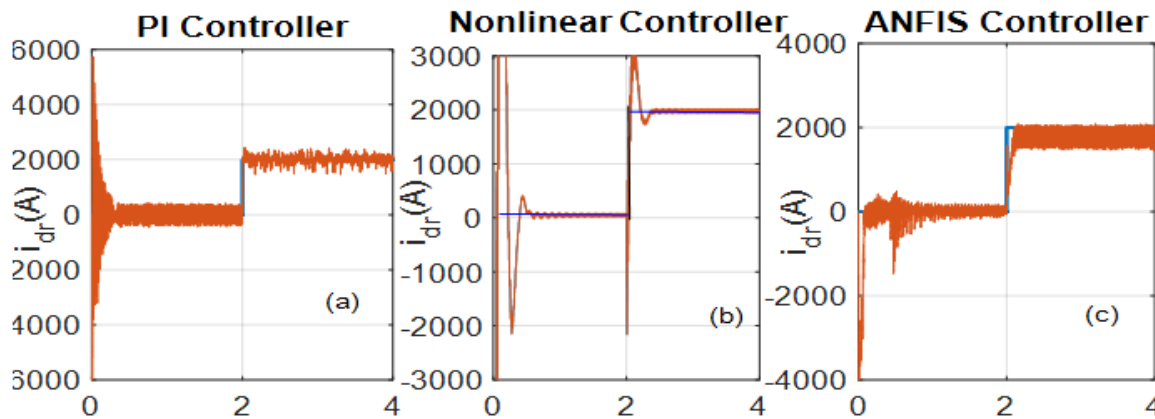


Fig. 10: Comparative d-axis rotor current tracking response for a step change in reactive power demand at t=2 sec: (a) PI, (b) Nonlinear, (c) AFIS

Table 3 shows the detailed comparison among controllers. The proposed AFIS controller shows comparatively better performance in terms of rotor speed convergence, dc bus voltage regulation and grid disturbance minimization whereas the computation

burden is high and d-axis current tracking performance is moderate compared to fixed gain PI and adaptive backstepping based nonlinear controllers.

Table 3: Performance comparison among the proposed controllers

Operating condition	Property	PI controller	ABN controller	AFIS based controller
Speed convergence characteristics	Speed settling time	Less than 0.2s	Less than 0.05s	Less than 0.15s
	Speed overshoot	3.5%	0.4%	0.6%
DC bus voltage convergence at variable wind flow	Voltage settling time	Less than 0.1s	Less than 0.05s	Less than 0.05s
	Voltage fluctuation	Low	High	Very low

d-axis rotor current at step rise in reactive power demand	Current settling time	Less than 0.1s	More than 0.5 s	Less than 0.2s
	Steady state error	Negligible	Negligible with very high overshoot	Marginal error with fluctuation
Computational burden	Block computation speed	Low	Medium	High
Ripple in grid currents at fixed wind speed		Lower than other controllers	Very high	High
Performance under Grid voltage disturbance		Good	Moderate	Better than others

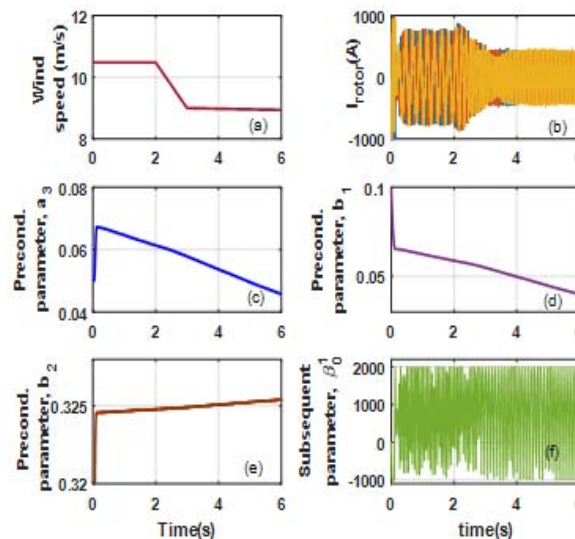


Fig. 11: Parameter updating pattern of online-tuned ANFIS scheme for variation in wind speed: (a) Changes in wind speed, (b) Frequency variation in rotor current, Variation in (c) precondition parameter,  $a_3$  (d) precondition parameter,  $b_1$  (e) precondition parameter,  $b_2$ , (f) subsequent parameter,  $\beta_0^1$

Figure 11 depicts the tuned parameters of the proposed algorithm along with the variation of the wind speed (Fig. 11(a)). The amplitude and frequency of the rotor current are shown in Fig. 11(b). Four parameters in the AFIS model are demonstrated in Fig. 11 ((c)-(f)). The variation of three preconditioned parameters,  $a_3$ ,  $b_1$  and  $b_2$  and one subsequent parameter is  $\beta_0^1$  is depicted. Hence, the adaptation of parameter in the proposed adaptive fuzzy inference system is proved from the figures.

## VI. CONCLUSION

Simplistic membership function based adaptive fuzzy scheme for DFIG operated WECS has been presented in this paper. The performance of the proposed controller has been investigated for grid-connected machine under different dynamic operating conditions. The simulation results suggest that the RSC controller regulates the power by adjusting the rotor speed and machine torque with the variation of wind speed. Also, the GSC controller is capable to maintain constant dc-link voltage and grid-current components

even after abrupt variation of the required power demand and wind speed. Comparative analyses have been performed among the proposed AFIS scheme, conventional fixed-gain PI controller and adaptive backstepping based nonlinear controller. The comparison outcomes suggest the superiority and robustness of the AFIS architecture-based controller in power regulation of DFIG based WECS.

### Conflict of Interest Statement

Authors declare that they have no known competing financial interests or personal relationships that could have appeared to influence the work reported in this paper.

## REFERENCES RÉFÉRENCES REFERENCIAS

1. Wang Q & Chang L, An intelligent maximum power extraction algorithm for inverter-based variable speed wind turbine systems, IEEE Transactions on Power Electronics, 19, 1242-1249, 2004.
2. Abdullah MA, Yatim AHM. & Tan CW, An online optimum-relation-based maximum power point tracking algorithm for wind energy conversion

- system, Australasian Universities Power Engineering Conference (AUPEC), Australia, 1-6, 2014.
3. Urtasun A, Sanchis P and Marroyo L, Small wind turbine sensorless MPPT robustness analysis and lossless approach, *IEEE Transactions on Industry Applications*, vol. 50, pp. 4113-4121, Nov. 2014.
  4. Yan R, Masood N, Saha TK, A new tool to estimate maximum wind power penetration level: In perspective of frequency response adequacy, *Applied Energy*, vol. 154, pp. 209–220, Sep 2015.
  5. Hui J, Bakhshai A, Jain P, A sensor-less adaptive maximum power point extraction method with voltage feedback control for small wind turbines in off-grid applications, *IEEE Journal Emerging on Selected Topic of Power Electronics*, vol. 3, pp.817-828, Sep. 2015.
  6. Abad G, López J, Rodríguez M, Marroyo L, Iwanski G, Doubly Fed Induction Machine, Modeling and Control for Wind Energy Generation, *IEEE Press Series on Power Engineering*, Wiley Publications, 2011.
  7. Tanaka T, Toumiya T and Suzuki T, "Output control by hill-climbing method for a small scale wind power generating system", *Renewable Energy*, vol. 12, pp.387-400, December 1997.
  8. Mendis N, Muttaqi KM, Sayeef S and Perera S, "Standalone operation of wind turbine-based variable speed generators with maximum power extraction capability", *IEEE Transactions on Energy Conversion*, vol. 27, no. 4, December 2012.
  9. Xiong P and Sun D, "Backstepping-based DPC strategy of a wind turbine-driven DFIG under normal and harmonic grid voltage", *IEEE Transaction on Power Electronics*, vol. 31, pp. 4216-4225, June 2016.
  10. Azzouz M, Elshafei AI and Emar H, "Evaluation of fuzzy-based maximum power-tracking in wind energy conversion systems", *IET Renewable Power Generation*, vol. 5, pp.422-430, Nov. 2011.
  11. Chen SZ, Cheung NC, Wong KC and Wu J, "Integral sliding-mode direct torque control of doubly-fed induction generators under unbalanced grid voltage", *IEEE Transactions on Energy Conversion*, vol. 25, pp. 356-368, June 2010.
  12. Sam SZ and Angel TS, "Performance optimization of PID controllers using fuzzy logic," 2017 IEEE International Conference on Smart Technologies and Management for Computing, Communication, Controls, Energy and Materials (ICSTM), 2017, pp. 438-442, doi: 10.1109/ICSTM.2017.8089200.
  13. Li H, Shi KL, McLaren PC, "Neural-network-based sensorless maximum wind energy capture with compensated power coefficient", *IEEE Transactions on Industry Applications*, vol. 41, no. 6, Dec. 2005.
  14. Jabr HM, Lu D and Kar NC, "Design and implementation of neuro-fuzzy vector control for wind-driven doubly-fed induction generator", *IEEE Transactions on Sustainable Energy*, vol. 2, no. 4, pp. 404-413, October 2011.
  15. Amin IK, Uddin MN and Marsadek M, "ANFIS based Neuro-Fuzzy Control of DFIG for Wind Power Generation in Standalone Mode," 2019 IEEE International Electric Machines & Drives Conference (IEMDC), 2019, pp. 2077-2082, doi: 10.1109/IEMDC.2019.8785334.
  16. Vrionis TD, Koutiva XI and Vovos NA, "A Genetic Algorithm-Based Low Voltage Ride-Through Control Strategy for Grid Connected Doubly Fed Induction Wind Generators," in *IEEE Transactions on Power Systems*, vol. 29, no. 3, pp. 1325-1334, May 2014, doi: 10.1109/TPWRS.2013.2290622.
  17. Labdai S, Hemici B, Nezli L, Bounar N, Boukroune A and Chrifi-Alaoui L, "Control of a DFIG Based WECS with Optimized PI controllers via a duplicate PSO algorithm," 2019 International Conference on Control, Automation and Diagnosis (ICCAD), 2019, pp. 1-6, doi: 10.1109/ICCAD46983.2019.9037879.
  18. Heydari A, Garcia DA, Fekih A, Keynia F, Tjernberg LB and De Santoli L, "A Hybrid Intelligent Model for the Condition Monitoring and Diagnostics of Wind Turbines Gearbox," in *IEEE Access*, vol. 9, pp. 89878-89890, 2021, doi: 10.1109/ACCESS.2021.3090434.
  19. Uddin MN, Amin IK, Rezaei N and Marsadek M, "Grey Wolf Optimization based Power Management Strategy for Battery Storage of DFIG-WECS in Standalone Operating Mode," 2018 IEEE Industry Applications Society Annual Meeting (IAS), 2018, pp. 1-7, doi: 10.1109/IAS.2018.8544633.
  20. Jang JSR., Sun CT, and Mizutani E, *Neuro-fuzzy and soft computing: a computational approach to learning and machine intelligence*, Upper Saddle River, NJ: Prentice Hall, 1997.
  21. Karray F and deSilver C, *Soft computing and intelligent systems design: theory, tools, and applications*, Pearson Publishing Inc., 2004.
  22. Chy MMI, Uddin MN, "Development and implementation of a new adaptive intelligent speed controller for IPMSM drive" *IEEE Transactions on Industry Applications*, vol. 45, no. 3, pp. 1106-115, May-June 2009.
  23. Amin IK, *Robust Control Techniques for DFIG Driven WECS with Improved Efficiency*, PhD dissertation, Dept. of Electrical Engineering, Lakehead University, Thunder Bay, ON, Canada, 2019.
  24. Amin IK and Uddin MN, "Nonlinear Control Operation of DFIG-Based WECS Incorporated With Machine Loss Reduction Scheme," in *IEEE Transactions on Power Electronics*, vol. 35, no. 7, pp. 7031-7044, July 2020, doi: 10.1109/TPEL.2019.2955021.